Journal of
Synchrotron
Radiation

ISSN 1600-5775

Received 24 May 2013
Accepted 1 November 2013

X-ray absorption near-edge structure anomalous behaviour in structures with buried layers containing silicon nanocrystals

V. A. Terekhov,[a]* D. I. Tetelbaum,[b] D. E. Spirin,[a] K. N. Pankov,[a] A. N. Mikhailov,[b] A. I. Belov,[b] A. V. Ershov[b] and S. Yu. Turishchev[a]

[a]Solid State Physics and Nanostructures Department, Voronezh State University, Universitetskaya pl. 1, Voronezh 394006, Russian Federation, and [b]Lobachevsky State University of Nizhni Novgorod, Pr. Gagarina 23, Nizhni Novgorod 603950, Russian Federation. *E-mail: ftt@phys.vsu.ru

Substructure and phase composition of silicon suboxide films containing silicon nanocrystals and implanted with carbon have been investigated by means of the X-ray absorption near-edge structure technique with the use of synchrotron radiation. It is shown that formation of silicon nanocrystals in the films' depth (more than 60 nm) and their following transformation into silicon carbide nanocrystals leads to abnormal behaviour of the X-ray absorption spectra in the elementary silicon absorption-edge energy region (100–104 eV) or in the silicon oxide absorption-edge energy region (104–110 eV). This abnormal behaviour is connected to X-ray elastic backscattering on silicon or silicon carbide nanocrystals located in the silicon oxide films depth.

Keywords: XANES; silicon nanocrystals; X-ray absorption inversion phenomenon.

1. Introduction

The formation of silicon nanocrystals (nc-Si) in a dielectric matrix that is luminescent in the visible-red and near infra-red ranges (1.4–1.8 eV) is one of the current areas of interest in opto- and nano-electronics (Pavesi & Turan, 2010). The luminescent band shift to short wavelengths, overlapping the whole visible range, can extend applications possibilities of silicon structures for different optoelectronics devices. It has been shown (see, for example, Zhao *et al.*, 1998; Gonzalez-Varona *et al.*, 2000; Perez-Rodriguez *et al.*, 2003; Tetelbaum *et al.*, 2009; Boryakov *et al.*, 2012) that simultaneous implantation of silicon and carbon ions into SiO_2 films leads to photoluminescence in the range from near infra-red to ultraviolet wavelengths due to the formation of silicon nanocrystals as well as carbon and silicon carbide nanocrystals. The luminescence extension to the visible and ultraviolet spectral range was realised by carbon ion implantation into SiO_x films on silicon substrates where the nanocrystalline silicon phase was formed as the non-stoichiometric oxide decomposition $SiO_x \rightarrow Si + SiO_2$ under high-temperature annealing (Belov *et al.*, 2010). By means of the X-ray photoelectron spectroscopy (XPS) technique it was found (Boryakov *et al.*, 2012; Belov *et al.*, 2010) that silicon atoms with Si 2*p* core-level binding-energy values close to crystalline SiC (100.8 eV; Dufour & Rochet, 1997) were located over the 70–170 nm surface layers of investigated samples. However, the absence of a sharp SiC peak in the XPS data mentioned above as well as the presence of low oxidation degree oxides at the same depth with silicon binding energies of ~100.5–101.2 eV (Himpsel *et al.*, 1988) argues against the proposition of silicon carbide formation. In the present work we attempted to investigate the same samples by means of the X-ray absorption near-edge structure (XANES) technique that is highly sensitive to the local surroundings of given atoms. Along with the confirmation of the SiC phase formation we detected spectral features that demonstrate the influence on XANES spectra of chemical bonds of those Si atoms that are located much deeper than the probing depth of the technique used. These spectral features are of common interest due to the application of the XANES technique in nanostructured systems studies.

2. Experimental details

Non-stoichiometric silicon oxide films (SiO_x) of thickness ~300 nm were formed on KDB-0.005 (111) and KDB-12 (100) silicon substrates using the technique described by Belov *et al.* (2010). Part of the sample was subjected to ion implantation of carbon. Then, irradiated samples as well as the initial ones were annealed at 1373 K in a nitrogen atmosphere for 2 h. Implantation doses (6×10^{16}, 9×10^{16}, 1.2×10^{17} cm^{-2}) and carbon ion energy (40 keV) were the same as those of Belov *et al.* (2010).

Samples were investigated by the XANES technique at the Synchrotron Radiation Center's Aladdin storage ring (University of Wisconsin-Madison, Stoughton, USA). Spectra registration near the Si $L_{2,3}$ absorption edge with 0.05 eV instrumental broadening was performed at the Mark V

beamline. Spectra registration near the *K* absorption edge of silicon was performed at the DCM beamline with 0.9 eV instrumental broadening. The radiation grazing angles for XANES detection were 90° if other values are not given. Sample drain current detection was used for XANES spectra registration using synchrotron radiation photon energy variations. Herewith the spectral dependence of the Auger and photoelectrons yield is detected from the sample surface. For the case of the common XANES technique this yield is proportional to the X-ray absorption coefficient in a thin surface layer whose thickness is determined by the atoms' energy structure and their surroundings (Rumsh *et al.*, 1961). As will be shown below under nanostructures investigation, the spectrum shape can depend on the structure and composition of layers that are deeper than the regular probing depth of the XANES technique, from which secondary electrons are not escaping directly.

3. Results and discussion

To analyze the chemical state of silicon in the investigated structures formed before and after carbon ion implantation as well as the annealed ones, let us consider the XANES data presented in Fig. 1 in the energy range of the silicon *K*-edge. For comparison, spectra of reference samples are presented in Fig. 2, *i.e.* silicon plate, thick amorphous silicon film, polycrystalline silicon carbide β-SiC, and amorphous films of SiO_2 with 10 nm and 100 nm thickness obtained by silicon thermal oxidation. The layer thickness, from photoelectrons and Auger electrons emitting in the considered energy range, is about 65 nm according to Kasrai *et al.* (1996). Besides the main elemental silicon maximum at 1841 eV in the spectra of reference silicon samples we also observe the 1847 eV feature that is connected to the presence of silicon oxide. For the thin 10 nm SiO_2 film, the elemental silicon peak observation (feature in Fig. 2) is caused by a c-Si substrate signal that is not detectable for the 100 nm SiO_2 film.

The main peak for the investigated unannealed SiO_x films is caused by a SiO_2 phase that follows from comparison of spectra given in Figs. 1 and 2. The shoulder (feature) '*a*' peculiar to the *K* absorption edge of elemental silicon (1841 eV) is observed in the low energy range of the given spectra indicating c-Si phase inclusions in the considered films. A relatively intensive shoulder '*b*' at 1844.2 eV is observed as well. We associate feature '*b*' with the presence of silicon atoms in the initial film with intermediate oxidation degree since the energy position of this shoulder is close to the mean value of the maxima for elemental Si and SiO_2 phases.

The relative intensities of the low-energy shoulders '*a*' and '*b*' mentioned above noticeably decrease after high-temperature annealing of the films. This is evidence of elemental silicon and non-stoichiometric oxide content decreasing within

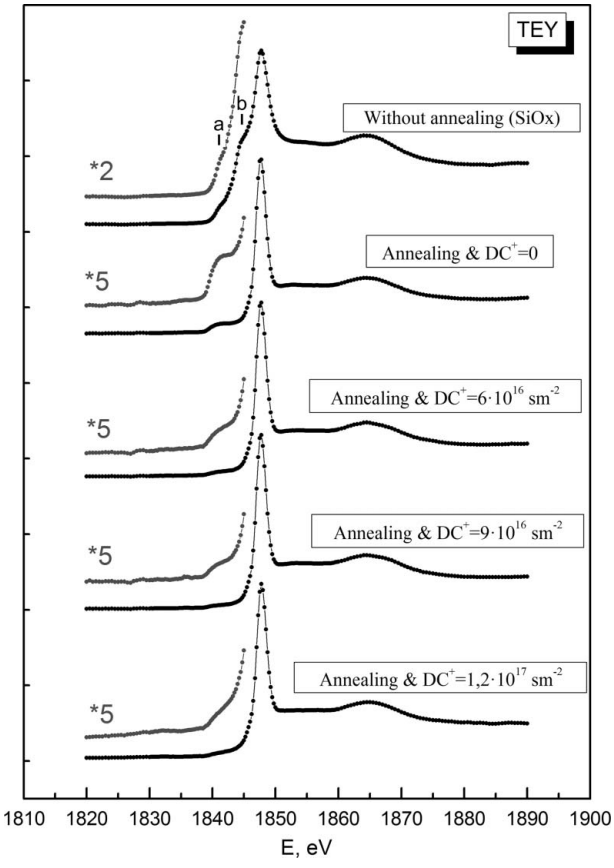

Figure 1
XANES *K*-edges of SiO_x/Si(111) structures with nc-Si.

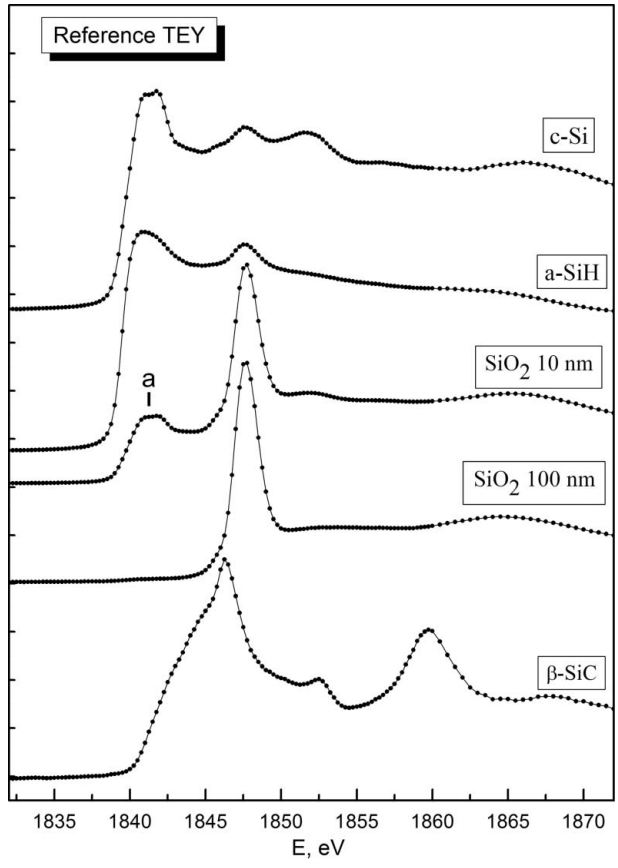

Figure 2
XANES *K*-edges of reference samples.

the analyzed layer. It was established earlier (Terekhov *et al.*, 2010) that thermal treatment identical to that considered in the present work led to stoichiometric SiO_2 formation in the 60 nm surface layer caused by the residual oxygen in the annealing atmosphere.

After C^+ ion implantation followed by annealing, a more noticeable decreasing of the elemental silicon feature (Fig. 1) is observed. This is in good agreement with XPS results that demonstrated an elemental silicon depth of occurrence $\geq$60 nm for annealed SiO_x films without carbon implantation (Terekhov *et al.*, 2011) and >70 nm after carbon ion implantation according to Belov *et al.* (2010). According to Pavesi & Turan (2010), the increase of the carbon implantation dose leads to an elemental silicon content decrease in the analyzed layer that is caused by reaction with implanted atoms. The shape changes of the low-energy-spectra tail (under energies lower than 1843.5 eV) with increase of implantation dose should be noted as well. Instead of a plateau at 1840–1843.5 eV that is well expressed in the case of the non-implanted sample, the spectral shape is transformed into an almost linear slope. Moreover, the spectral intensity at ~1843.5 is increased under the ultimate implantation dose (1.2×10^{17} cm^{-2}). This transformation can be connected to silicon carbide formation because SiC XANES at the Si *K*-edge has a maximum at 1846 eV and a continuous shoulder falling down with energies up to 1840 eV (Fig. 2).

Let us proceed to the results of silicon $L_{2,3}$ absorption spectra investigations. Fig. 3 shows XANES spectra for the investigated structures formed on (111) substrates before and after carbon ion implantation, and Fig. 4 shows XANES Si $L_{2,3}$ data for measured 'references': c-Si, SiO_2 and β-SiC. At the Si $L_{2,3}$ absorption edge XANES (TEY) the sampling depth is known to be about 5 nm (Kasrai *et al.*, 1996). Since the reference samples c-Si and β-SiC had a natural SiO_2 layer on their surface the observed spectral features at 106 and 108 eV (Fig. 4) are due to this oxide layer. As can be easily seen from Fig. 3 in the case of the initial film, we observed a spectrum that is typical of the stoichiometric SiO_2. As shown above for the Si *K*-edges, this is evidence of near-surface thin SiO_x layer oxidation to SiO_2 that took place while the samples were stored in the ambient air.

After annealing of the not-implanted film in the energy range beginning at 100 eV (that corresponds to the absorption edge of elemental silicon), an abnormal 'inverse' spectrum shape is observed: instead of the usual sample drain current rising with the increase of photon energy, a decrease of the spectrum relative intensity is observed forming a dip in the 100–104 eV range. The same behaviour has been observed

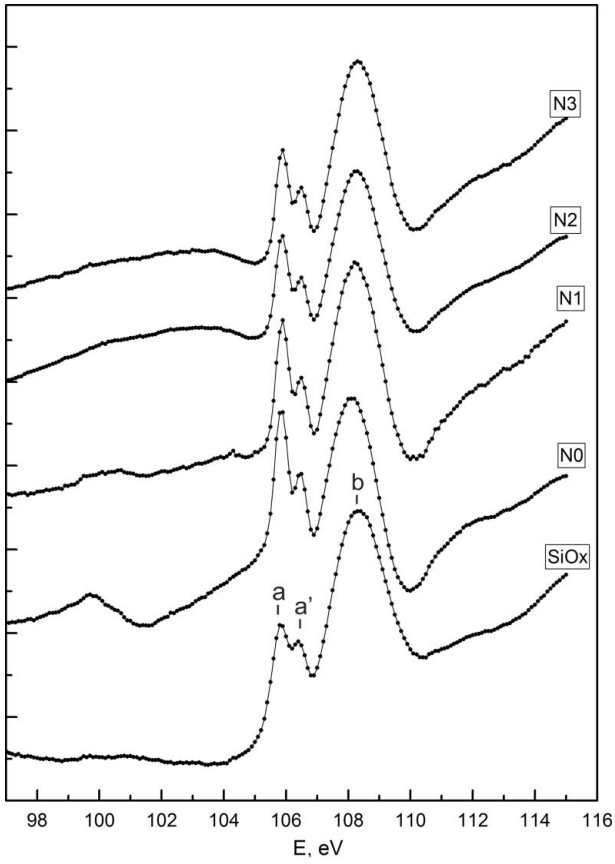

Figure 3
Si $L_{2,3}$ XANES for SiO_x/Si(111) structures with nc-Si. SiO_x: initial film. N0: film without implantation and after annealing. N1: film after implantation with a dose of 6×10^{16} cm^{-2} and following annealing. N2: film after implantation with a dose of 9×10^{16} cm^{-2} and following annealing. N3: film after the implantation with a dose of 1.2×10^{17} cm^{-2} and following annealing.

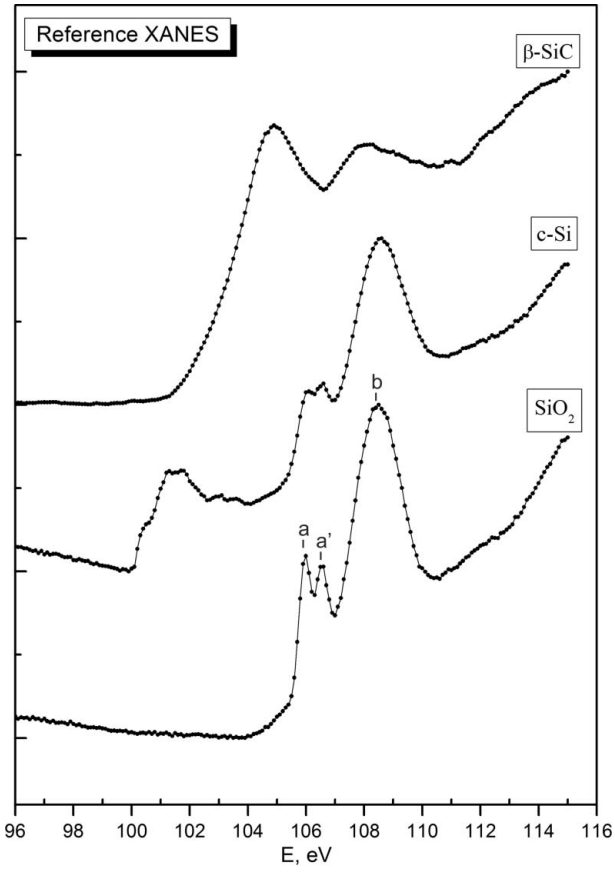

Figure 4
XANES $L_{2,3}$-edges of reference samples.

previously (Terekhov *et al.*, 2010) for sputtered and annealed SiO_x films. Terekhov *et al.* (2010) explained this phenomenon by the actual proportion of the electron yield from the sample that is registering in the XANES technique to the X-ray beam electromagnetic field in the near-surface layer from which electrons are emitted. The electromagnetic field intensity in this layer is determined not only by the X-ray quanta flux falling but also by the backscattered flux from deeper layers. In the case of nanosized inclusions present in the considered layer, which are different from the matrix by structure and composition, the backscattered beam amplitude and phase in turn are determined by the following processes: photon elastic scattering, absorption of the falling and backscattered beams, reflection (generally multiple) on internal heteroboundaries and possible interference. In the case of a nanocomposite structure any of these factors can be found to be strongly dependent on the elemental and phase composition, the nanosized inclusions concentration, size and morphology, and even more on their depth distribution. Under those quanta energies where ionization of certain atomic shells appears to be possible (where rising sample drain current is observed in the case of homogeneous single-phase samples), in the nanocomposite system a TEY rise is possible as well as a TEY decrease depending on the relative contribution of the different factors (mentioned above). Apparently, in the case of the investigated system, the main reason for the Si $L_{2,3}$ range dip formation is the weakening of quanta back flow near the surface as a result of an intensification of the absorption of the initial and backscattered beams by silicon nanocrystals located under the surface SiO_2 layer (with energies sufficient for Si $L_{2,3}$ shell ionization). Moreover, in the XANES dip formation for the absorption-edge range of atoms that are forming nanoparticles, the phenomenon of anomalous elastic scattering (Hoperskii & Yavna, 2002) can make a significant contribution. For the case where the photon energy coincides with the core-level ionization energy, this phenomenon's cross section has a sharp minimum.

The XANES spectra inversion disappeared in the case of samples obtained on (111) substrates and measured after carbon implantation with and without annealing (Fig. 3). Small traces of the inversion remained under the lowest carbon doses as a small feature observed in the 99–101 eV range. This inversion disappearance indicates a change in the phase compositions (and also optical properties) of the films. Herewith the elemental silicon that is contained in the nanocrystals is bonding with carbon.

Let us turn to the XANES spectra analysis for films formed on silicon substrates with (100) orientation given in Fig. 5. For C^+-implanted samples these spectra are different from those taken for films obtained on the (111) silicon substrates in the 100–105 eV energy range. As demonstrated for (111) substrates under lowest C^+ implantation dose (6×10^{16} cm^{-2}), the inversion phenomenon connected to the elemental silicon formation disappeared in the 100–105 eV energy range with only some traces left at ~100 eV, shown as a kink. However, in contrast to the (111) substrate orientation case the dip (inversion) is observed in the 105–112 eV energy range. The

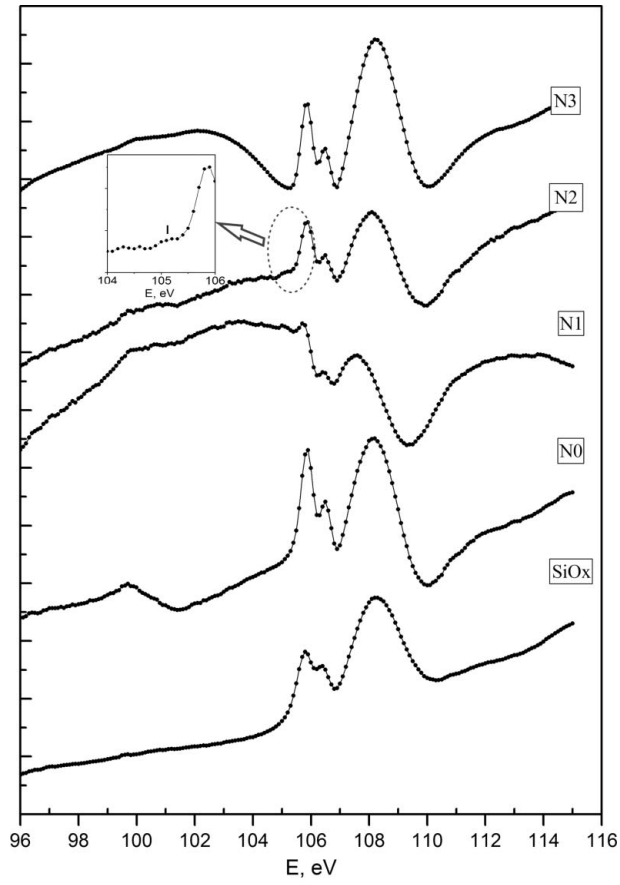

Figure 5
Si $L_{2,3}$ XANES for SiO_x/Si(100) structures with nc-Si. SiO_x: initial film. N0: film without implantation and after annealing. N1: film after implantation with a dose of 6×10^{16} cm^{-2} and following annealing. N2: film after implantation with a dose of 9×10^{16} cm^{-2} and following annealing. N3: film after implantation with a dose of 1.2×10^{17} cm^{-2} and following annealing.

peaks observed in this range for reference samples and the initial SiO_x film formed on the silicon substrate are caused by silicon bonds with oxygen in SiO_2. With an increasing C^+ implantation dose, this inversion becomes less expressed and under the 1.2×10^{17} cm^{-2} dose spectra regain their normal shape in the considered energy range. Under the 6×10^{16} cm^{-2} carbon implantation dose the inversion also appears to be less expressed under decreasing radiation grazing angle and the spectrum shape is becoming closer to the 'regular' one (Fig. 6). Since variation of the radiation grazing angle leads to a variation of the effective depth for radiation interaction with the film material, the latter observation confirms that the observed spectrum inversion phenomenon is connected to the structural and phase conditions of the films layers that are placed outside the oxidized layer formed as a result of the anneal. It should be noted that for the sample with the lowest implantation dose under all grazing angles used for Si $L_{2,3}$ spectra registration (Figs. 5 and 6) the noticeable feature is observed under quanta energy ~105 eV that corresponds to the main maximum position of the silicon carbide spectrum (Fig. 4). This is further evidence of the presence of the latter compound in the SiO_2 film studied. The spectral feature

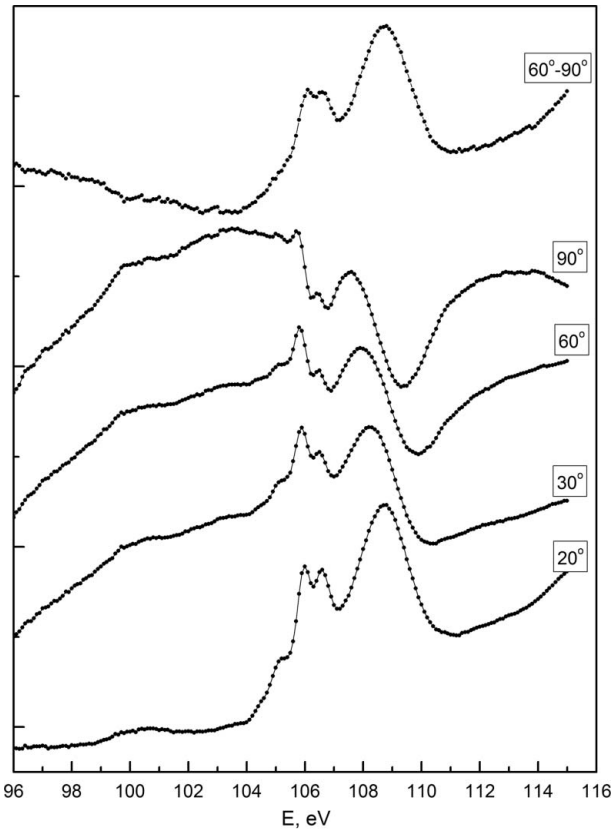

Figure 6
Si $L_{2,3}$ XANES spectra for the N1 sample (implantation dose 6×10^{16} cm^{-2}) formed on the (100) substrate registered at different grazing angles, and the difference spectrum for 60° and 90° registration.

appears to a lesser degree for the sample with the greater carbon implantation dose of 9×10^{16} cm^{-2} (Fig. 5). This can be due to the predominant formation of carbon inclusions instead of SiC.

In the same way as we used above to explain the observation of the 100–105 eV spectral feature inversion phenomenon, it can be considered that the inversion in the 105–112 eV range is caused by nanostructures peculiarities that affect the behaviour of the backscattered beam (Vinogradov, 1989). X-ray quanta absorption with energies relevant to the $L_{2,3}$-edge of silicon atoms bonded to oxygen and carbon leads to the attenuation of backscattered X-ray photons that weaken the electron yield intensity in turn and register as a dip in the spectrum. It should be noted that reference spectra extremes that are caused by the β-SiC phase are placed in the same range as those of silicon dioxide (see Fig. 5). The important role of deep layers in the observed phenomenon is visually demonstrated by the difference curve for the spectra registered under 90° and 60° grazing angles (Fig. 6). This curve almost coincides with the 'regular' SiO_2 absorption spectrum (Fig. 4). This is connected to the low contribution from depths containing formed nanoparticles in the difference spectrum.

The fact that we did not observe the spectrum inversion any time we registered spectra from nanostructures suggests that the inversion can take place only under certain criteria that are connected to the structural–phase conditions of the backscattering X-ray quanta layer. For example, we did not observe any inversions near the Si $L_{2,3}$ absorption edge (Terekhov *et al.*, 2007) where studied SiO_2:nc-Si structures were obtained under Si^+ ion implantation into SiO_2. Also, silicon nanocrystals in SiO_2:nc-Si structures were formed not only at films depths but also in the near-surface layers, leading to the absence of the intermediate 'pure' SiO_2 layer. Thus specific criteria that lead to the inversion phenomenon are a subject for more detailed studies.

What is the reason for such spectra behaviour and the dependence on substrate orientation? We have demonstrated (Terekhov *et al.*, 2012) that in similar samples silicon nanocrystals are not oriented chaotically and their predominant orientation coincides with that of the substrates used. Apparently the crystal orientation affects the optical properties of the considered nanostructures due to the anisotropy of the optical constants that leads to the intensity differences observed for backscattered X-rays.

4. Conclusion

The results obtained reveal that for XANES data interpretation for nanostructured systems it is necessary to consider the contribution of the (falling) direct X-ray beam as well as the backscattered one. On the one hand, this fact makes the interpretation of spectra more complicated; on the other, it creates additional diagnostic possibilities for the structure of such systems and morphology analysis by the non-destructive XANES technique. The practical realisation of these opportunities requires additional research.

The results obtained confirm the formation of silicon carbide nanosized inclusions under the carbon ion implantation of SiO_x films.

The study was supported by The Ministry of Education and Science of Russia, project No. 14.132.21.1682. This work is based in part upon research conducted at the Synchrotron Radiation Center, University of Wisconsin-Madison, which is supported by the National Science Foundation under award No. DMR-0537588.

References

Belov, A. I., Mikhaylov, A. N., Nikolitchev, D. E., Boryakov, A. V., Sidorin, A. P., Gratchev, A. P., Ershov, A. V. & Tetelbaum, D. I. (2010). *Semiconductors*, **44**, 1450–1456.
Boryakov, A. V., Nikolitchev, D. E., Tetelbaum, D. I., Belov, A. I., Ershov, A. V. & Mikhaylov, A. N. (2012). *Phys. Solid State*, **54**, 394–403.
Dufour, G. & Rochet, F. (1997). *Phys. Rev. B*, **56**, 4266–4282.
Gonzalez-Varona, O., Perez-Rodriguez, A. & Garrido, B. (2000). *Nucl. Instrum. Methods Phys. Res. B*, **904**, 161163.
Himpsel, F. J., McFeely, F. R., Taleb-Ibrahimi, A., Yarmoff, J. A. & Hollinger, G. (1988). *Phys. Rev. B*, **38**, 6084–6096.
Hoperskii, A. N. & Yavna, V. A. (2002). *X-ray Photon Anomalous Elastic Scattering by an Atom.* Rostov-On-Don: SKNC VSh. (In Russian.)
Kasrai, M., Lennard, W. N., Brunner, R. W., Bancroft, G. M., Bardwell, J. A. & Tan, K. H. (1996). *Appl. Surf. Sci.* **99**, 303–312.

Pavesi, L. & Turan, R. (2010). Editors. *Silicon Nanocrystals: Fundamentals, Synthesis and Applications*, p. 648. Weinheim: Wiley-VCH.

Perez-Rodriguez, A., Gonzalez-Varona, O., Garrido, B., Pellegrino, P., Morante, J. R., Bonafos, C., Carrada, M. & Claverie, A. J. (2003). *Appl. Phys.* **94**, 254.

Rumsh, M. A., Lukirskii, A. P. & Shchemelev, V. N. (1961). *Izv. Akad. Nauk SSSR Ser. Fiz.* **25**, 1060.

Terekhov, V. A., Tetelbaum, D. I., Zanin, I. E., Pankov, K. N., Spirin, D. E., Mikhailov, A. N., Belov, A. I. & Ershov, A. V. (2012). *Izv. Vys. Uch. Zav. Mater. El. Tech.* **4**, 54–59. (In Russian.)

Terekhov, V. A., Turishchev, S. Yu., Kashkarov, V. M., Domashevskaya, E. P., Mikhailov, A. N. & Tetel'baum, D. I. (2007). *Physica E*, **38**, 16–20.

Terekhov, V. A., Turishchev, S. Yu., Pankov, K. N., Zanin, I. E., Domashevskaya, E. P., Tetelbaum, D. I., Mikhailov, A. N., Belov, A. I. & Nikolichev, D. E. (2011). *J. Surf. Invest.* **5**, 958–968.

Terekhov, V. A., Turishchev, S. Yu., Pankov, K. N., Zanin, I. E., Domashevskaya, E. P., Tetelbaum, D. I., Mikhailov, A. N., Belov, A. I., Nikolichev, D. E. & Zubkov, S. Y. (2010). *Surf. Interface Anal.* **42**, 891–896.

Tetelbaum, D. I., Mikhaylov, A. N., Vasiliev, V. K., Belov, A. I., Kovalev, A. I., Wainstein, D. L., Mendeleva, Yu. A., Finstad, T. G., Foss, S., Golan, Y. & Osherov, A. (2009). *Surf. Coat. Tech.* **203**, 2658–2663.

Vinogradov, A. V. (1989). *X-ray Mirror Optics.* Leningrad: Mashinostroenie. (In Russian.)

Zhao, J., Mao, D. S. & Lin, Z. X. (1998). *Appl. Phys. Lett.* **73**, 1838.